

CHAPTER 76

INCORPORATION OF WAVE EFFECTS IN A 3D HYDROSTATIC MEAN CURRENT MODEL

H.J. de Vriend¹⁾ and N. Kitou²⁾

Abstract

The consistency of the mathematical formulation of a 3D hydrostatic current model for coastal areas is discussed. At various points, widely accepted concepts and formulations are shown to lead to inconsistencies, and more consistent alternatives are proposed. Besides, some essential lacunae in our physical knowledge of 3D wave-driven currents are indicated.

Introduction

Nearshore currents have a three-dimensional structure, which plays an important part in coastal dynamics. Mathematical models in this field ought to take this into account. Especially if the wave-induced "cross-shore" sediment transport is concerned, descriptions of the near-bed current velocity based on a 2D depth-integrated current model will fail (cf. De Vriend, 1986). Also 2D-vertical models will fail in many practical cases, by lack of longshore uniformity. Quasi-3D models, coupling a 1D-vertical and a 2D depth-integrated model to describe a 3D current field, may bring relief here. This type of models, however, needs further substantiation before being ready to describe nearshore currents (Arcilla et al., 1990; Svendsen and Putrevu, 1990). Fully 3D current models, therefore, have their part to play here, if it were only as a reference for simpler models (e.g. Q3D).

The present paper describes the incorporation of wave-effects into a 3D-hydrostatic mean current model. It concerns the form and the consistency of the basic mathematical formulation, rather than the actual numerical implementation.

Model concept

We will start from a 3D hydrostatic current model, with the vertical plane mapped onto a rectangle via the so-called sigma-trans-

-
- 1) DELFT HYDRAULICS, P.O.B. 152, 8300 AD Emmeloord, The Netherlands
 - 2) Demokritos Univ. of Xanthi, Dept. of Civil Engrg., 67100 Xanthi, Greece

formation. It is essential for the concept presented herein, that the vertical is discretized into a fixed number of steps (layers), the uppermost of which covers at least the full height of the sea waves (Fig. 1).

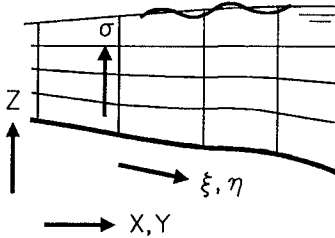


Fig. 1 Discretization of the vertical plane

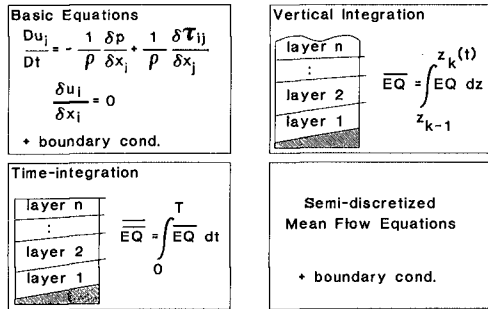


Fig. 2 Derivation of semi-discretized wave-averaged equations

The net wave effects are included in the constituting equations for the mean current by formal integration of the Reynolds equations over the vertical elements of the computational grid and over the time scale of the waves (Fig. 2).

The resulting semi-discretized equations contain a number of wave residual terms, viz.

- mass flux terms in the equation of continuity,
- mass flux terms in the momentum equations, and
- wave-induced effective stresses in the momentum equations.

Besides, the waves influence the turbulent exchange of momentum and the effective bottom shear stress.

In the next sections, we will discuss these effects one by one, supposing the wave parameters to be given, i.e. we will not go into the matter of fully interactive wave-current systems.

Wave-induced mass flux

In the case of periodic waves, the wave-averaged equation of continuity contains no net wave-effects in layers entirely below the wave trough level, i.e. in all layers but the one adjacent to the water surface.

The wave-averaged equation for this top layer reads

$$\frac{\partial \Delta_k}{\partial t} + \frac{\partial}{\partial X_i} \left(U_{i,k} \Delta_k + \frac{M_i}{\rho} \right) + T.T. = 0 \tag{1}$$

in which:

- t = time,
- X_i = horizontal co-ordinates (i=1,2),
- Δ_k = thickness of the k-th layer,

- $U_{i,k}$ = horizontal mean velocity components, averaged over the k-th layer,
- M_i = wave-induced mass flux components,
- ρ_i = mass density of the fluid,
- T.T. = terms related to the sigma-transformation.

The wave-induced mass flux components in this equation are defined by

$$M_i = \frac{1}{T} \int_t^{t+T} dt \int_{z_{n-1}}^{z_n} \rho \tilde{u}_{i,n} dz \tag{2}$$

in which T denotes a significant time scale of the wave motion, long enough to yield a meaningful average, $\tilde{u}_{i,n}$ is the wave orbital velocity in the top layer, and n is the index of this layer.

On the basis of a wave theory, Eq. (2) can be elaborated in terms of wave field parameters (height, direction, etcetera). We will discuss this in a later section.

At the physical level, Eq. (2) means an extension with respect to 2D-vertical and 2D-horizontal situations: the mass flux can give rise to 3D circulations, as is illustrated in Fig. 3.

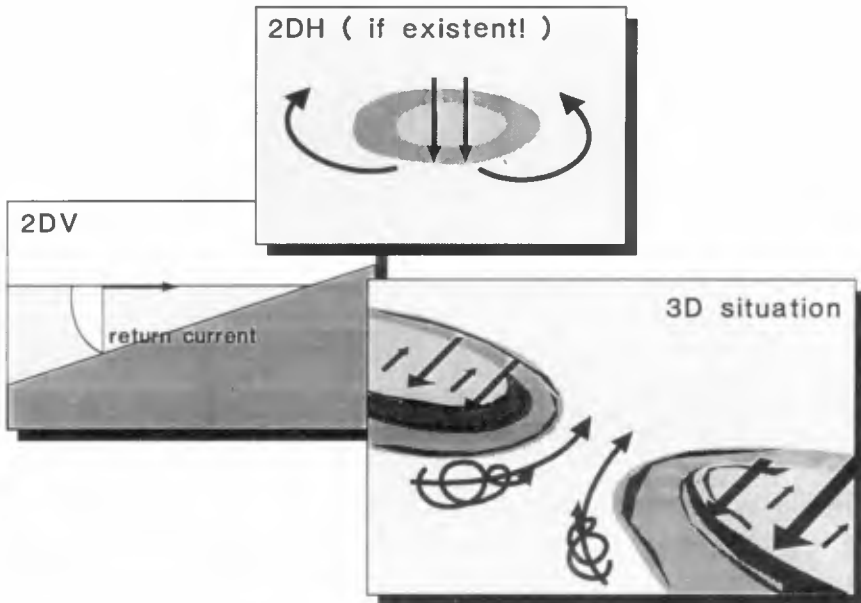


Figure 3 3D effect of wave-induced mass flux

Wave-induced momentum flux

The procedure outlined in Figure 2, when applied to the momentum equations, yields residual wave-effects through the non-linear advection terms. Using

$$\frac{1}{T} \int_t^{t+T} dt \int_{z_{k-1}}^{z_k} u_{i,k} u_{j,k} dz = U_i U_j \Delta_k + U_i \frac{M_i}{\rho} + U_j \frac{M_j}{\rho} + \frac{1}{T} \int_t^{t+T} dt \int_{z_{k-1}}^{z_k} \tilde{u}_{i,k} \tilde{u}_{j,k} dz \quad (3)$$

we can split the residuals of the horizontal advection terms into a mean-flow part, a mass-flux related part (two terms), and a part that contributes to the radiation stress.

The vertical advection term also yields a wave-residue, which should not be disregarded a priori (also see Svendsen and Lorenz, 1989, and Deigaard and Fredsøe, 1989).

The resulting semi-discretized equation for the k-th layer reads

$$\begin{aligned} \frac{D}{Dt} \left(U_{i,k} \Delta_k + \frac{M_i}{\rho} \right) + (U_i W)_{z_{k-1}}^{z_k} = & \\ - g \Delta_k \frac{\partial z_s}{\partial X_i} + \frac{1}{\rho} \frac{\partial}{\partial X_j} (\Delta_k \bar{\tau}_{ij,k}) + \frac{\bar{\tau}_{i,z}}{\rho} \Big|_{z_{k-1}}^{z_k} + & \\ + \frac{1}{\rho} \frac{\partial}{\partial X_j} (\Delta_k \bar{\sigma}_{ij,k}) - \langle \tilde{u}_i \tilde{w} \rangle \Big|_{z_{k-1}}^{z_k} + T.T. & \end{aligned} \quad (4)$$

in which:

W = mean vertical velocity component,

g = acceleration due to gravity,

z_s = water surface level,

$\bar{\tau}_{ij}$ = Reynolds stress components in vertical planes,

$\bar{\tau}_{i,z}$ = Reynolds stress components in horizontal planes,

$\bar{\sigma}_{ij}$ = wave-induced effective stress,

\tilde{u}_i, \tilde{w} = wave-orbital velocity components,

T.T. = terms due to the co-ordinate transformation.

The mass flux component, non-zero in the top layer only, is defined by (2). The definition of the wave-induced effective stress reads

$$\bar{\sigma}_{ij,k} = \frac{1}{T} \int_t^{t+T} \frac{dt}{\Delta_k} \int_{z_{k-1}}^{z_k} \rho \tilde{u}_{i,k} \tilde{u}_{j,k} dz + \frac{\delta_{ij}}{T} \int_t^{t+T} \frac{dt}{\Delta_k} \int_{z_{k-1}}^{z_k} (\bar{p} - \rho \langle \tilde{w}^2 \rangle) dz \quad (5)$$

in which \bar{p} denotes the instantaneous hydrostatic part of the pressure and δ_{ij} is the Kronecker delta.

In general, the wave-induced mass flux will be small as compared with the mass flux related to the mean flow. If not, the mean flow velocity will be so small, that the advection terms are negligible, anyway. We will therefore disregard the mass-flux related residual advection terms.

The remaining residue of wave-induced horizontal advection basically acts as an effective stress, comparable to the Reynolds stress. In depth-integrated models, it adds up to the radiation stress (Longuet-Higgins and Stewart, 1964); in the present 3D model, this stress is distributed over the vertical. Consequently, the wave-induced current forcing, composed of the divergence of the effective stress and the vertical advection residue, also has a vertical distribution.

In addition to the wave-induced terms in (4), which vanish in the absence of waves, there are also wave-influenced terms, which are just modified by wave effects. The shear stress terms are of this type, and so are the near-bed boundary conditions.

In the next sections, we will discuss how the mass flux, the effective stress and the wave-induced current forcing can be elaborated in terms of global wave field properties, such as energy density, energy dissipation rate, etcetera. The other wave-influenced terms will receive further attention in a later section.

Evaluation for harmonic waves

Wave-induced mass flux

Using linear wave theory, Eq. (2) for the wave-induced mass flux can easily be elaborated to

$$M_i = \frac{E}{c} e_i^w \quad (6)$$

in which E is the energy density of the wave field, c is the wave celerity, and e_i^w denotes the components of the unit vector in the direction of wave propagation.

Wave-induced forcing ("classical" approach)

In depth-integrated models, it is customary to evaluate the radiation stresses on the basis of linear wave theory for a quasi-uniform domain (mild-slope approximation).

When applied to the present vertically resolved model, this theory yields for the effective stresses

$$\begin{aligned} \bar{\sigma}_{ij,k} &= \left(N - \frac{1}{2}\right) E f_{ij}(z_k) + \frac{1}{2} \delta_{kn} E \\ \langle \tilde{u}_{i,k} \tilde{w} \rangle &= 0 \end{aligned} \quad (7)$$

in which N is the ratio of group and phase celerity, and f_{ij} is a function of z only. Note that the last term of the expression for $\bar{\sigma}$ exists only in the top layer.

The corresponding wave-induced driving force per unit area (henceforth called "force", as the term "stress" has already been used for the effective stress tensor) can be elaborated to

$$F_{i,k} = \frac{D}{c} e_i^w f_D(z_k) - \frac{1}{2} \frac{\partial E}{\partial X_i} f_E(z_k) + \dots \tag{8}$$

in which D denotes the dissipation rate of the wave field, and f_D and f_E are functions of z only.

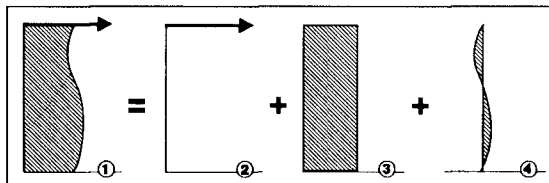


Figure 4 Decomposition of wave-induced force ("classical" theory)

The wave-induced force according to (8) can be split into three parts, viz. (also see Fig. 4)

- a surface part: $F_{s_i} = - \frac{1}{2} \frac{\partial E}{\partial X_i}$ (9)

- a depth-invariant part: $\bar{F}_i = h \frac{\partial}{\partial X_i} \left\{ \frac{(n-\frac{1}{2})E}{h} \right\} + \frac{1}{2} \frac{\partial E}{\partial X_i}$ (10)

- a depth-varying part: $F_{z_i} = \frac{E}{h} f_1(z) + \frac{1}{2} \frac{\partial E}{\partial X_i} f_2(z) + \frac{D}{c} f_3(z)$ (11)

The depth-invariant part of the force is fundamentally unable to drive a circulation current and is therefore disregarded here. The depth-varying part is basically able to drive a circulation, but it is usually assumed weak enough to be disregarded. This leaves the surface part, which acts at the mean water surface like a wind stress. It corresponds with the force at the wave trough level in various undertow models (Svendsen, 1984; Stive and Wind, 1986).

According to Eq. (9), the force will be non-zero in non-breaking (e.g. shoaling) wave fields. This is a major inconsistency of the model. If there is no ambient current and no wave breaking, all of the above results stem from a description of an ideal fluid in irrotational motion. The surface force resulting from this theory, however, will give rise to an infinite vorticity when applied to an ideal fluid body.

Wave-induced forcing (revised theory)

In a genuinely uniform situation, there will be no gradients in global parameters, such as E, and hence there will be no surface force and no inconsistency. From a practical point of view, however, a model should cover more than this trivial case.

Any deviation from uniformity in the "classical" model gives rise to the aforementioned inconsistency. Upon closer investigation, this is basically due to the assumption of quasi-uniformity of the domain and the global wave field parameters, which underlies the description of the vertical structure of the wave motion in the "mild-slope" approximation (Berkhoff, 1976):

$$\begin{Bmatrix} \tilde{\eta} \\ \tilde{u} \\ \tilde{p} \end{Bmatrix} = \begin{Bmatrix} \hat{\eta} \\ \hat{u}(z) \\ \hat{p}(z) \end{Bmatrix} \cos\chi \quad \text{with: } \chi = \omega t - kX \quad (12)$$

$$\tilde{w} = \hat{w}(z) \sin\chi$$

In this approximation, each of the amplitude functions \hat{u} , \hat{p} and \hat{w} is strictly similar in every vertical of the domain. Spatial non-uniformities only affect their scaling.

In order to achieve consistency of the model, we shall relax the mild-slope approximation. Going back to irrotational motion in a domain with a mildly sloping bottom and weakly non-uniform global wave parameters, we can take the classical solution as a basis and perturb this for small non-uniformities. In a horizontally 1D case, oriented along the X-axis, this yields in a first-order approximation (see De Vriend and Kitov, 1990, for further details)

$$\tilde{\eta} = \hat{\eta} \cos\chi \quad (13)$$

$$\tilde{u} = \hat{u}(z) \cos\chi + f_u \left(\frac{\partial z_b}{\partial X}, \frac{\partial z_s}{\partial X}, \frac{\partial k}{\partial X}, \frac{\partial \hat{\eta}}{\partial X}; z \right) \sin\chi \quad (14)$$

$$\tilde{w} = \hat{w}(z) \sin\chi + f_w \left(\frac{\partial z_b}{\partial X}, \frac{\partial z_s}{\partial X}, \frac{\partial k}{\partial X}, \frac{\partial \hat{\eta}}{\partial X}; z \right) \sin\chi \quad (15)$$

in which the functions f_u and f_w depend linearly on the gradients of the global parameters z_b , z_s , w_k and $\hat{\eta}$.

Substituting this result into the expressions for the effective stresses yields

$$\bar{\sigma}_{ij,k} = (N-1/2) E f_{ij}(z_k) + \frac{1}{2} \delta_{kn} E \quad (16)$$

$$\langle \tilde{u}_{i,k}, \tilde{w} \rangle = (N-1/2) E f_E \left(\frac{\partial z_b}{\partial X}, \frac{\partial z_s}{\partial X}, \frac{\partial k}{\partial X}; z \right) + f_E(z) \frac{\partial E}{\partial X} \quad (17)$$

in which f_{ij} and f_E are functions of z only, and f_E depends linearly on the gradients of z_b , z_s and k . Note that, unlike Eqs. (14) and (15), the effects of the amplitude variation are separated and yield the energy-gradient term of (17).

Also note that (16) is identical to (7), i.e. in a first-order approximation the residue of the horizontal momentum flux is not affected by the global non-uniformities.

In contrast with the classical theory, however, the vertical momentum flux is deviating from zero now!

Although we have only derived the revised theory for a 1-D case, it seems reasonable to assume, that similar results will be found when applying the same idea to horizontally 2-D situations.

Let us therefore assume, without formal proof, that in such a situation the vertical momentum flux contribution (17) can simply be rotated into the direction of wave propagation.

In that case, elaboration of the wave-induced driving forces yields

$$F_{i,k} = \frac{D}{c} e_i^w f_D(z_k) + \text{irrot. terms} \quad (18)$$

The irrotationality of the last terms in this equation refers primarily to the horizontal plane, but, upon closer inspection, these terms are also irrotational (uniformly distributed) in the vertical. Hence this part of the force is basically unable to drive a circulation current and can be disregarded here. The remaining part is proportional to the energy dissipation rate of the wave field (cf. Longuet-Higgins, 1970; Battjes, 1988), and it turns out to be concentrated in the top layer, where the $\langle \tilde{u}\tilde{w} \rangle$ -term reaches its highest value and where the dissipation actually takes place (Fig. 5).

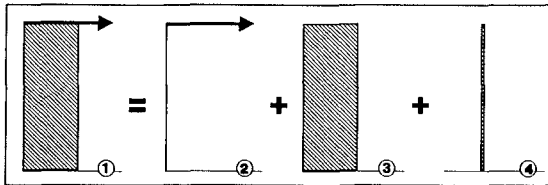


Figure 5 Decomposition of wave-induced force (revised theory)

The inconsistency of the classical model has now been removed: if the flow is inviscid, there is neither dissipation, nor wave-induced current forcing. Apparently, the vertical momentum flux term, which is the only part of the forcing influenced by the present extension of the wave model, plays a key role in achieving consistency (cf. Svendsen and Lorenz, 1989, for waves on a sloping bottom, and Deigaard and Fredsøe, 1989, for breaking waves). This may seem to be in contrast with Stive and Wind's (1986) observation, that the $\langle \tilde{u}\tilde{w} \rangle$ -term, when evaluated on the basis of measured data, is relatively small. We would like to point out, however, that the principal effect of this term is concentrated in the top layer of the fluid, between the troughs and the crests of the waves. Stive and Wind's data set does not extend to this area.

Role of bottom friction and wind-input

Although the formal derivation of (18) is based on the inviscid flow assumption, the wave boundary layer can easily be included. There, again, the $\langle \tilde{u}\tilde{w} \rangle$ -term plays a prominent part (Longuet-Higgins, 1953; also see Craik, 1982): it yields the driving force of the boundary layer streaming.

In general, the forcing will be located where the dissipation of organized motion actually takes place (cf. Nairn et al., 1990). As illustrated by Fig. 6, this will be in the surface layer for wave-breaking and wind-input (negative dissipation!), in the bottom boundary layer for bottom friction, and probably throughout the water column for wave-turbulence interaction in an ambient turbulent flow.

It may be clear, that in a depth-integrated current model outside the surf zone the contributions of the various types of wave energy dissipation ought to be weighted according to their location in the vertical. They cannot simply be piled up in a current-driving body force, which is implicitly assumed (via the assumptions under-

lying the depth-averaging) to be uniformly distributed over the vertical. This would imply too much emphasis on the forcing associated with bottom friction, and too little on the wind-induced forcing. Unfortunately, this is exactly what is done when putting the results of a wave model, including effects of wind-input and bottom friction, into a classical radiation stress and wave-induced force computation, and driving a depth-averaged current model with the resulting forces. Models of this type covering large areas with mainly non-breaking waves should therefore be considered with caution.

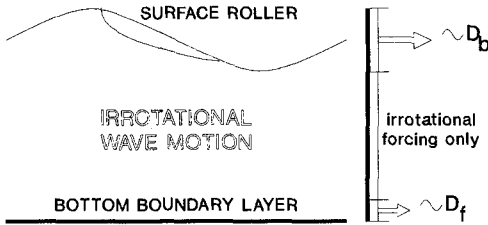


Figure 6

Location of wave-induced current forcing

Evaluation for broken waves

Roller concept

According to a concept introduced by Svendsen (1984), a broken wave of the spilling type can be considered as a harmonic carrier wave with a surface roller at its front face. This roller introduces an additional complication for the surf zone.

Since the roller moves with the wave celerity c , its contributions to the wave-averaged fluxes of mass, momentum and energy are given by (also see Deigaard and Fredsoe, 1989)

$$\text{mass flux: } \rho \frac{Ac}{\lambda} \tag{19}$$

$$\text{momentum flux: } \rho \frac{Ac^2}{\lambda} \tag{20}$$

$$\text{energy flux: } \rho \frac{Ac^3}{\lambda} \tag{21}$$

where λ denotes the wave length and A the cross-sectional area of the roller. According to Svendsen (1984), the latter quantity can be estimated at $0.9 H_{cw}^2$, if H_{cw} is the height of the carrier wave.

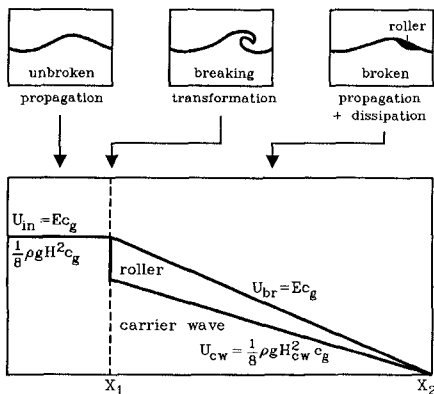
The total mean energy flux due to a broken wave follows from

$$E_{br}c_g = \frac{1}{8} \rho g H_{cw}^2 c_g + \rho \frac{Ac^3}{\lambda} \tag{22}$$

in which c_g is the group celerity of the waves. With the above approximation of A and the shallow water approximation of the phase and group celerities, this leads to (cf. De Vriend and Stive, 1987)

$$E_{br} = E_{cw} \left(1 + 7 \frac{h}{\lambda} \right) \tag{23}$$

Both (22) and (23) express, that there is a difference between the energy contents of the carrier wave and the broken wave as a whole, due to the contribution of the roller (Fig. 7).



Hence it makes a difference, whether we describe the waves by their bulk energy density, e.g. by solving an energy balance equation including a dissipation term, or by the height of the carrier wave, e.g. via a breaker height criterion. In the former case, the roller effect is already included in the computed energy density, E_{br} , whereas in the latter case the roller contribution has to be accounted for explicitly.

Figure 7 Energy flux due to broken waves

Wave-induced mass flux

The wave-induced mass flux, found by adding the contributions of the carrier wave and the roller, reads

$$M_{br} = \frac{E}{c} + \rho \frac{Ac}{\lambda} \tag{24}$$

or, making use of Eq. (23) and the underlying assumptions,

$$M_{br} = \frac{E_{br}}{c} \tag{25}$$

Apparently, the mass flux, at least in this approximation, can be expressed in terms of the bulk energy density of the broken waves, without any additional term to account for the roller contribution.

Note, however, that this is only valid as long as the shallow water approximation applies to c and c_g .

Wave-induced forcing

Eq. (18) gives the wave-induced forces in terms of the energy dissipation rate, including the effect of breaking. Hence, it is the most convenient to derive these forces from a wave model that describes the decay of the bulk energy density by solving an energy balance equation including dissipation. In that case, the roller contribution in D needs not be calculated explicitly.

If the wave model describes the height of the carrier wave, e.g. via the breaker height criterion $H_{br} = yh$, the dissipation rate has to be calculated from

$$D = - \frac{\partial}{\partial X} \left[\frac{1}{8} \rho g H_{cw}^2 c_g + \rho \frac{Ac^3}{\lambda} \right] \tag{26}$$

Here the roller contribution has to be taken explicitly into account.

Wave influence on turbulence effects

Waves also exert their influence on the mean current through turbulence and boundary shear stress. Non-breaking waves affect the

near-bed water motion and the bed shear stress (for instance, see Van Kesteren and Bakker, 1984, or Davies et al., 1988), and they are also suspected to interact with the turbulence higher up in the water column.

Broken waves introduce an additional turbulence production mechanism, which can be of significant influence in a large part of the vertical (Justesen et al., 1986), and possibly also in the horizontal (Wind and Vreugdenhil, 1986).

In the transition zone, where waves start breaking, there is a transformation of organized wave motion, through overtopping and roller formation, into turbulence. Nairn et al. (1990) show, that this transition process should be taken into account when modelling the currents in this zone.

Starting from the Boussinesq hypothesis, so from a scalar eddy viscosity, there is a range of turbulence models and bed stress models at our disposal. Very few of these models, however, include wave effects in a well-validated manner.

Without going into details, we will consider three types of models, indicate how wave effects can be included and assess the state of the art.

Partial-slip model

Leendertse (1987), in his 3D-hydrostatic current model, uses a combination of a constant eddy viscosity and a partial-slip condition at the bottom

$$\nu_t \left. \frac{\partial U}{\partial z} \right|_{z_b} = A |U_1| U_1 \quad (27)$$

in which the factor A is the key element of the model. It has to be derived from known shear stress descriptions, such as Chezy's or Manning's model.

This technique, sometimes referred to as Bazin's method, has proved rather successful in plane or slightly disturbed steady shear flow (e.g. in rivers and well-mixed estuaries; Engelund, 1974). As far as we know, it has never been shown to work equally well for strongly distorted oscillatory shear flow.

When attempting to apply this concept to the coastal situation, with its strongly distorted 3D flow and its complex shear stress relationships, the determination of A becomes rather laborious, if possible, at all. In view of the rather weak physical basis, the effort to further work out this concept seems not justified.

Algebraic eddy viscosity model

Algebraic eddy viscosity models are widely used in engineering applications. Very often, this is combined with a similarity assumption, which, for a simple pressure-driven shear current, boils down to

$$\nu_t = \bar{\nu}_t f_v(z) \quad (28)$$

A parabolic shape function f_v , combined with appropriate boundary conditions, leads to the well-known logarithmic velocity profile. The depth-invariant scaling factor, $\bar{\nu}_t$, reflects the turbulence production mechanism. In plane shear flow, for instance, $\bar{\nu}_t$ is proportional to the bottom shear velocity.

A way of including wave effects into this type of model is to adjust \bar{v}_t for wave-induced turbulence generation. In principle, this can concern only turbulence generated at the bottom, since other production mechanisms are likely to correspond with other vertical shape functions. This means, that breaker-generated turbulence is not included, nor the interaction of waves and turbulence throughout the water column.

It may be possible to model the various wave-effects on turbulence separately and to superimpose the results. The eddy viscosity is a non-physical artefact, which is unsuited for superposition, but superimposing turbulence kinetic energy contributions seems a defensible case (Deigaard et al., 1986).

At the eddy viscosity level, this would mean a quadratic composition

$$v_t = \left[\left\{ \bar{v}_t f_v(z) \right\}_{\text{bottom}}^2 + \left\{ \bar{v}_t f_v(z) \right\}_{\text{breaking}}^2 + \dots \right]^{\frac{1}{2}} \quad (29)$$

shear

In practical model applications, a vertical resolution which is sufficient to describe the details of boundary layers is seldomly feasible. In those models, the boundary layer is described with a separate, semi-analytical boundary layer model, which is matched with the numerical solution, e.g.

$$U = \frac{U_*}{\kappa} \ln \frac{z}{z_0} \quad (30)$$

in which U_* denotes the wall shear velocity and z_0 is the point of zero intersection of the velocity profile. In general, z_0 is given in terms of roughness parameters, and the matching with the numerical model goes via U_* .

Waves are known to influence both quantities: they tend to enhance the effective wall shear stress, and they shift the point of zero intersection of the mean velocity further away from the wall (see, for instance, Van Kesteren and Bakker, 1984).

Higher-order turbulence closure

A more sophisticated way of describing turbulence is the so-called higher-order closure, based on one or more coupled transport equations for turbulence properties, such as the kinetic energy. Typical examples are the k-model (e.g. Deigaard et al., 1986) and the k- ϵ model (e.g. Wind and Vreugdenhil, 1986).

Higher-order turbulence models have proven their value for intra-wave current modelling (e.g. Davies et al., 1988). At the level of wave-averaged current modelling, however, their present applicability is limited by a lack of basic knowledge. Possibly important turbulence production mechanisms (wave-turbulence interaction) are still poorly known, and the knowledge of the intra-wave processes has hardly been parameterized in terms of mean-current and global wave properties.

On the other hand, depth-averaged models including wave breaking as a source of turbulence production (Battjes, 1983; Wind and Vreugdenhil, 1986) seem to work well. It has to be pointed out, however, that these models have only been tested critically for the inner surf zone, where this type of production is predominant.

For other areas, wave-averaged higher order turbulence models have not yet been substantiated.

Conclusions

The principal conclusions from the work presented herein can be summarized as follows.

- The wave-induced mass flux has to be included in the equation of continuity for the top layer. It will not always be compensated by a return current in the same water column, but can give rise to 3D circulations.
- The $\langle \bar{u}\bar{w} \rangle$ -term in the wave-averaged momentum equation plays an essential part in the consistency of the model in spatially non-uniform situations.
- The classical mild-slope approximation leads to inconsistency of the model, because it yields inappropriate estimates of the $\langle \bar{u}\bar{w} \rangle$ -term. An extended linear wave model for mildly non-uniform situations leads to consistent results.
- Wave-induced current forcing is located there, where the wave energy dissipation actually takes place. This means, that the forcing due to spilling breakers takes place near the water surface, and that forcing associated with bottom dissipation takes place near the bottom.
- The necessity to include a roller contribution when modelling wave-driven currents depends on whether the bulk energy density of the breaking waves is described, or the carrier wave height. Only in the latter case, a roller contribution has to be taken explicitly into account.
- So far, the application of higher-order turbulence models in wave-averaged current models is not supported by sufficient physical knowledge, except maybe for very specific situations.

Acknowledgement

The major part of the work presented herein was carried out during the second author's stay at DELFT HYDRAULICS, in 1988, which was co-financed by the University of Xanthi, Greece. The results will be implemented and utilized by both authors in Project 0035-C, "G6 Coastal Morphodynamics" of the Marine Science and Technology (MAST) Programme of the Commission of the European Communities.

References

- Arcilla, A.S., Collado, F.R., Lemos C.M. and Rivero, F., 1990. Another quasi-3D model for surfzone flows. Proc. 22nd ICCE, Delft (in press).
- Battjes, J.A., 1983. Surf zone turbulence. Proc. XXth IAHR-Congr., Moscow. Sem. "Hydrodynamics of waves in coastal areas".
- Battjes, J.A., 1988. Surf zone dynamics. Ann. Rev. Fluid Mech., 20, p. 257-293.
- Berkhoff, J.C.W., 1976. Mathematical models for simple harmonic linear water waves; wave diffraction and refraction. Doct. thesis, Delft Univ. of Techn., 103 pp.
- Craik, A.D.D., 1982. The drift velocity of water waves. J. Fluid Mech., 116, p. 187-205.

- Davies, A.G., Soulsby, R.L. and King, H.L., 1988. A numerical model of the combined wave and current bottom boundary layer. *J. Geoph. Res.*, 93,C1, p. 491-508.
- Deigaard, R., Fredsøe, J. and Hedegaard, I.B., 1986. Suspended sediment in the surf zone. *J. Waterway, Port, Coastal, Ocean Engrg.*, 112,1, p. 115-128.
- Deigaard, R. and Fredsoe, J., 1989. Shear stress distribution in dissipative water waves. *Coastal Engrg.*, 13, p. 357-378.
- De Vriend, H.J., 1986. 2DH computation of transient sea bed evolutions. Proc. 20th ICCE, Taipei, Taiwan, p. 1689-1712.
- De Vriend, H.J. and Kitou, N., 1990. Incorporation of wave effects in a 3D hydrostatic current model. Delft Hydraulics, Rept. H 1295 (in preparation).
- De Vriend, H.J. and Stive, M.J.F., 1987. Quasi-3D modelling of near-shore currents. *Coastal Engineering*, 11,5&6, p.565-601.
- Engelund, F., 1974. Flow and bed topography in channel bends. Proc. ASCE, Jnl. Hydr. Div., 100,HY11, p. 1631.
- Justesen, P., Fredsoe, J. and Deigaard, R., 1986. The bottle-neck problem for turbulence in relation to suspended sediment transport in the surf zone. Proc. 20th ICCE, Taipei, p. 1225-1239.
- Leendertse, J.J., 1987. A three-dimensional alternating direction implicit model with fourth order dissipative non-linear advection terms. Rijkswaterstaat, Rept. WD-3333-NETH.
- Longuet-Higgins, M.S., 1953. Mass transport in water waves. *Phil. Trans. Royal Soc.*, A254, p. 535-581.
- Longuet-Higgins, M.S., 1970. Longshore currents generated by obliquely incident waves. *J. Geoph. Res.*, 75, p. 6778-6801.
- Longuet-Higgins, M.S. and Stewart, R.W., 1964. Radiation stresses in water waves; a physical discussion with applications. *Deep Sea Res.*, 11, p. 529-562.
- Nairn, R.B., Roelvink, J.A. and Southgate, H.N., 1990. Transition zone width and implications for modelling surfzone hydrodynamics. Proc. 22nd ICCE, Delft, (in press).
- Stive, M.J.F. and Wind, H.G., 1986. Cross-shore mean flow in the surf zone. *Coastal Engineering*, 10, p. 325-340.
- Svendsen, I.A., 1984. Mass flux and undertow in the surf zone. *Coastal Engineering*, 8, p. 303-329.
- Svendsen, I.A. and Lorenz, R.S., 1989. Velocities in combined undertow and longshore currents. *Coastal Engrg.*, 13, p. 55-79.
- Svendsen, I.A. and Putrevu, U., 1990. Nearshore circulation with 3-D current profiles. Proc. 22nd ICCE, Delft, (in press).
- Van Kesteren, W.G.M. and Bakker, W.T., 1984. Near bottom velocities in waves with a current; analytical and numerical computations. Proc. 19th ICCE, Houston, p. 1161-1177.
- Wind, H.G. and Vreugdenhil, C.B., 1986. Rip-current generation near structures. *J. Fluid Mech.*, 171, p. 459-476.